Praise Worthy Prize

International Review of Mechanical Engineering (I.RE.M.E.), Vol. 12, N. 2
ISSN 1970 - 8734 *February 2018*

Active Flow Control by Suction on Vehicle Models with Variations on Front Geometry

Rustan Tarakka[1], Nasaruddin Salam[1], Jalaluddin[1], Muhammad Ihsan[2]

Abstract – *Current development of modern vehicles requires rigorous aerodynamic study due to the complexity of the flow field around a car which is influenced by geometric design of vehicles. That makes research on the aerodynamic drag force on vehicles very important. This study aimed to analyze the effect of active flow control by suction and variations on front geometry towards the reduction of aerodynamic drag as well as pressure coefficients on vehicle models. The research was conducted in computational and experimental approaches. Frontal slant angle variations (θ) of 25°, 30° and 35° were applied in the study. Computational approach used k-epsilon standard turbulence model. Upstream and suction velocity values used were16.7 m/sand 0.5 m/s, respectively. Load cells were used in the experimental approach to validate the reduction of aerodynamic drag obtained from computational approach. Results indicate that active flow control by suction and variations on front geometry give significant impact to the increasing on pressure coefficients and the reduction of aerodynamic drag on vehicle models. While the largest increasing on pressure coefficients occurred on the vehicle model with θ=35° at 26.50%, the largest reduction of aerodynamic drag occurred on the same model with the value of 14.74 for computational approach and 13.57 for experimental approach, while the reductions of aerodynamic drag coefficients of the two approaches differ about 1.17%.*

Keywords: *Aerodynamic Drag Reduction, Pressure Coefficients, Front Geometry, Suction, Vehicle Model*

Nomenclature

Cd	Drag coefficient
Cp	Pressure coefficient
Fd	Pressure drag force [N]
h	Height of test model [m]
l	Length of test model [m]
ρ	Density [kg/m^3]
θ	Front slant angle [^{o}]
Re	Reynolds number
S	Cross section area [m^2]
τ_w	Wall shear stress [N/m^2]
U_{sc}	Suction velocity [m/s]
U_o	Upstream velocity [m/s]
μ	Viscosity [N s/m^2]
w	Width of test model [m]

I. Introduction

In many developing countries with high population levels, the growth rate of passenger vehicle production has increased significantly, making the transport sector the world's major fuel oil user.

The amount of fuel consumption of motor vehicles such as the type of family vehicle is influenced by the magnitude of the aerodynamic drag force experienced by the vehicle.

Therefore, the reduction of aerodynamic drag force becomes a solution to achieve fuel efficiency. For most road vehicles, improvements to the wake flow characteristics could give significant drag reduction. The main contributions to aerodynamic drag arise from separated flows in the rear, causing pressure recovery losses and the creation of vortex in the wake [1]-[5].

In addition, the current development of modern vehicles also requires rigorous aerodynamic study due to the complexity of the flow field around a car that is influenced by the geometric design of the car. This makes research on the aerodynamic drag force on the vehicle very important. Therefore, the current research related to the subject has been conducted extensively [6], [7], [8], [9].

In earliest studies in the field of vehicle aerodynamics, simple vehicle models that can produce relevant features in the flow around real vehicles were mostly employed [1], [10], [11], [12], [13], [14]. One of the techniques under development to reduce aerodynamic drag on vehicles is by adding an active flow control. The active control strategy involves the addition of energy which aims to control (prevent or delay) the occurrence of flow separation that may lead to backflow on the surface of the vehicle without changing the shape of vehicles [15].

Many active control techniques have been developed by focusing on local intervention in wall turbulence deal

 https://doi.org/10.15866/ireme.v12i2.13876

with steady blowing or suction [16], [17], [18]. Brunn A. et al. [19] conducted numerical and experimental research on active controls on generic model vehicles. In this study, the generic vehicle model uses the basic design of the Ahmed model that has a size of ¼ of the original Ahmed body geometry. The investigated Ahmed 3D model had a slope angle on the back 25° and 35°. Numerical analysis in this study used LES turbulence model. The experimental and numerical approaches using constant blowing show that the resulting vortices become weak. However, overall the total drag change obtained is very small, only about 2.5% due to the weakening of vortices and increasing the separation flow region on the slant side of the Ahmed model.

Rouméas et al. [15] conducted numerical research using the Ahmed model as a test model with a slant angle of 25° to the horizontal reference. Continuous suction is a flow control which is used and placed on the back side of the fastback car. The results show that the effect of the suction provides reattachment effect on the smoothed stream on Ahmed body slant wall with 17% drag force reduction. Harinaldi et al. [20] conducted research using a modified/reversed Ahmed body. The model was equipped with active flow control by suction. Drag reduction obtained by 24% for computational approach and 14.8% for experimental approach. This study aimed to analyze the effect of active control by suction and variations on front geometry towards the reduction aerodynamic drag on vehicle models. Better reduction of aerodynamic drag can reduce flow separation that will lead to energy efficiency. The understanding of aerodynamic drag reduction and pressure coefficient are expected to improve the design method of future vehicles.

II. Methodology

The study investigates the drag reduction occuring in a bluff body of van model adapted from Ahmed model, in which flow streams in reversed direction to the original model (reversed Ahmed model) [20], [21], [22], [23]. The van model was equipped with an active control by applying suction. Reversed Ahmed body model was used because it represents a typical form of family van commonly produced by car manufacturer. The van model was used both in the computational methods (CFD) and experimental.

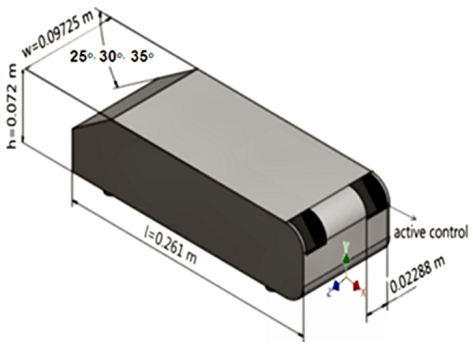

Fig. 1. Vehicle model *"reversed Ahmed model"*

Figure 1 shows the vehicle model used in the investigation. The geometric ratio of van model employed in the study to the original Ahmed body model [1] was 0.25.

Hence, the vehicle model geometry was defined by its length (l = 0.261m), width (w = 0.09725 m) and its height (h = 0.072 m). In this configuration, the front part of body was inclined with slant angles (θ) of 25°, 30°and 35° to the horizontal reference.

The amount of viscous drag force and pressure drag force F_d is presented in following equation:

$$F_d = \int \tau_w \sin\theta dS + \int p \cos\theta dS \quad (1)$$

Drag coefficient C_d is expressed as:

$$C_d = \int \frac{\tau_w}{\frac{1}{2}\rho V_\infty^2 S} \sin\theta dS + \frac{\int C_p \cos\theta dS}{S} \quad (2)$$

where $\tau_w = \mu(du/dy)_w$ is the wall shear stress which is evaluated from the velocity gradient at the wall and $C_p = (p\text{-}p_\infty)/(\rho V_\infty^2/2)$ is pressure coefficient which is evaluated from pressure distribution at the wall.

The 3D computational domain is shown in Figure 2 with dimensions of length (L) = 8l, width (W) = 2l, and height (H) = 2l (l = length of model in x-axis). Type of meshing was tetra/hybrid element with hex core type. The boundary condition was inlet velocity of 16.7 m/s.

Average free stream at far upstream region was assumed in a steady state and uniform condition. The suction velocity was set 0,5 m/s. Reynolds number corresponding to the length of the test model was Re = 2.98×10^5. The details of computational conditions are given in Table I.

TABLE I
COMPUTATIONAL CONDITION

Computational condition		
Vehicle model	3D, steady state θ=25°, θ=30° and θ=35°	
Fluid	Air	
Fluid properties	Density	1.225 kg/m^3
	Viscosity	0.000017894 kg/m-s
Boundary condition without active flow control	Vehicle model	Wall
	Pressure outlet	Pressure outlet
	Velocity inlet	Velocity inlet
	Wall	Wall
Boundary condition with active flow control by suction	Vehicle model	Wall
	Pressure outlet	Pressure outlet
	Velocity inlet	Velocity inlet
	Wall	Wall
	Suction1	Velocity inlet
	Suction2	Velocity inlet
Upstream velocity	16.7 m/s	
Suction velocity	0.5 m/s	

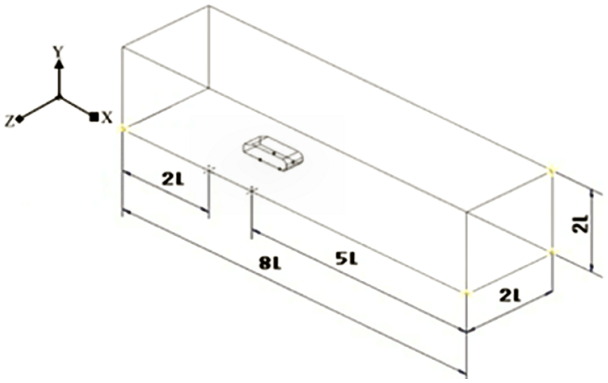

Fig. 2. The 3D computational domain

The model experimental tests were carried out in a controlled low speed wind tunnel. The tests employed van model made of acrylic material with a 0.25 scale to the original Ahmed body model [1]. The van models consisted of two test models which were model without flow control and model with active flow control by suction. The suction was configured inside the body of the model at the area where the flow separation was predicted to cause a significant drag based on the computational results. The suction was conducted by using a vacuum pump. Suction velocity was set at 0.5 m/s. Both models were placed in a low speed wind tunnel test section with free stream air flow.

The parameter to be investigated was the aerodynamic drag force measured by using a load cell as shown in Fig. 3. The measurement scheme of aerodynamic drag force is as shown in Fig. 4.

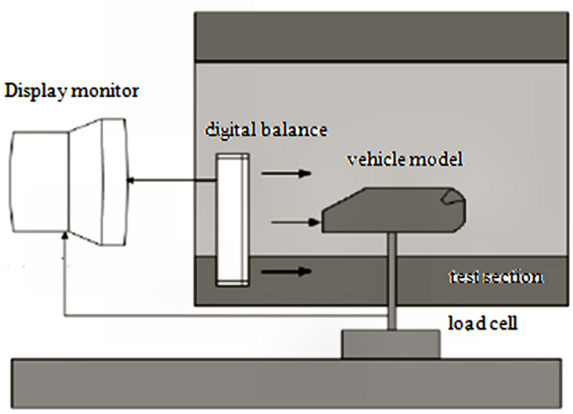

Fig. 3. Sketch of vehicle model placement to the load cell and calibration

Before the main experiments, the load cell was calibrated using a digital balance and then a preliminary measurement was performed to determine the statistical uncertainty of force measurement. The statistical uncertainty was predicted at about ± 2%.

Dimensionless drag coefficient related to drag force acting on the bluff body is then defined as follow:

$$C_d = \frac{F_d}{\frac{1}{2}\rho V_\infty^2 S} \quad (3)$$

where, ρ is air density, V_∞ is free stream velocity, S is cross sectional area and F_d is total drag force which works on vehicle models measured by a load cell.

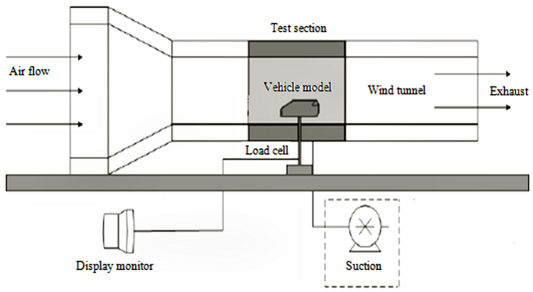

Fig. 4. Experimental setup for the aerodynamic drag force measurement

III. Results and Discussion

Patterns of pressure coefficient distribution are presented in the form of graphs of y/h toward C_p. The ratio y/h is the ratio of height of grid to height of vehicle model while C_p is the pressure coefficient. It is also shown in the graph lines that expressed pressure coefficient distribution patterns of rear part of vehicle models on z/w direction, where z/w is the ratio of width of grid to the width of vehicle models. Figures 5 show pressure coefficient distribution (C_p) on rear part of vehicle models with variations of slant angle (θ) of 25°, 30°and 35° and upstream velocity of 16.7 m/s.

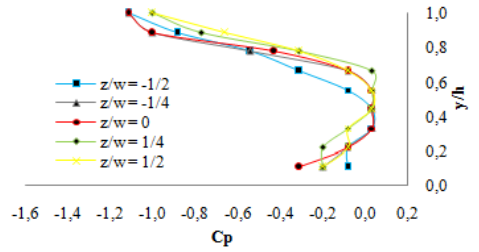

(a) θ = 25°

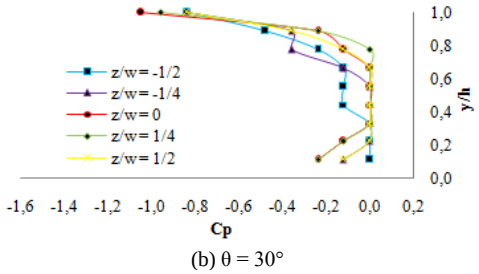

(b) θ = 30°

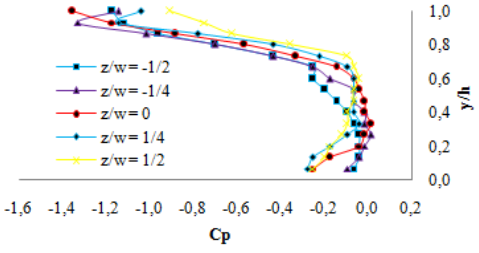

(c) θ = 35°

Figs. 5. Pressure coefficient distribution without active flow control

TABLE II
THE MINIMUM VALUE OF PRESSURE COEFFICIENT WITHOUT ACTIVE FLOW CONTROL

Vehicle model	Pressure coefficient, Cp	y/h	z/w
$\theta=25^0$	-1.1148	1	-1/4 and 0
$\theta=30^0$	-1.0716	1	0
$\theta=35^0$	-1,3556	1	0

Table II shows minimum values of pressure coefficients on respective test model. Minimum values of pressure coefficients of models occurred at y/h=1, at the edge of upper side of rear part of respective vehicle models. With variations of slant angle of each vehicle models, it is shown that the largest pressure coefficient occurred on vehicle model with slant angle on front part of 30° compared to that on models with 25° and 35° slant angles.

Flow separation occurring on rear part of vehicle models will cause back flow on the rear part of vehicle models and in turn will cause reduction of pressure coefficient. The phenomenon has confirmed research conducted by Anderson et al. [24].

Figures 6 show the distributions of pressure coefficients with upstream speed U_o = 16.7 m/s and suction speed U_{sc} = 0.5 m/s on the vehicle model with the slant angle at the front of 25°, 30° and 35° respectively.

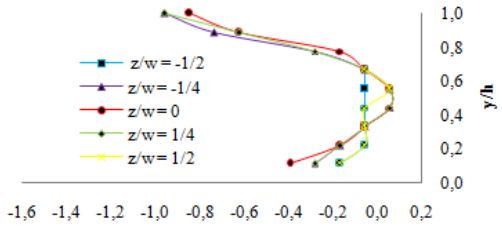

(a) θ = 25°

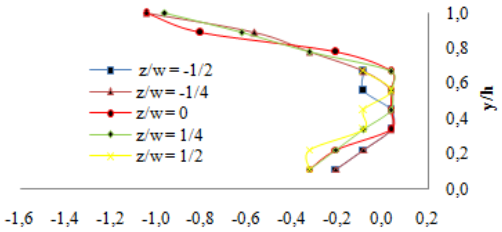

(b) θ = 30°

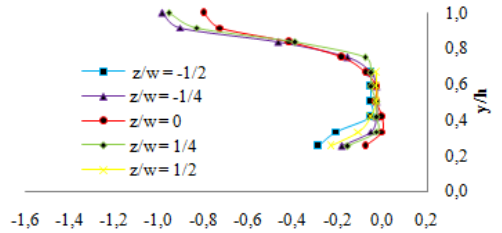

(c) θ = 35°

Figs. 6. Pressure coefficient distribution with active flow control by suction

Figure 6 shows that with the active control suction, the value of the pressure coefficient has increased. The value of the pressure coefficient changes positively at y/h = 0.6 to y/h = 1.

This shows that on the upper side of the rear part of each test model there is an increasing of pressure coefficient.

With the active control of suction, the low pressure stream due to shape factor and air friction with the test model wall can be reduced so that the flow separation can also be reduced or kept away from the rear part of the test model.

The minimum values of the pressure coefficient distribution with suction velocity U_{sc} = 0.5 m/s and upstream velocity U_o = 16.7 m/s are summarized in Table III.

Table III shows that the pressure coefficient distribution in each vehicle model with the variation of slant angle at the front was the smallest on the test model with a 30° front slant angle relative to the test model with 25° and 35° slant angle.

TABLE III
THE MINIMUM VALUE OF PRESSURE COEFFICIENT WITH ACTIVE FLOW CONTROL BY SUCTION

Vehicle model	Pressure coefficient, Cp	y/h	z/w
$\theta=25^0$	-0.9616	1	-1/4 and 1/4
$\theta=30^0$	-1.0442	1	0 and -1/4
$\theta=35^0$	-0.9964	1	-1/4

Table IV shows that the effect of additional active control by suction with U_{sc} = 0.5 m/s can reduce the flow separation at the rear of each vehicle model. Reduced separation of the flow will increase the pressure coefficients occurring in each vehicle model [25].

The effect of adding active control by suction which increases the test pressure coefficient occurs in all vehicle models. The largest increasing percentage of pressure coefficient with the addition of active control by suction occurred in the test model with the slant angle of the front of 35° at 26.50%.

TABLE IV
INCREASING PRESSURE COEFFICIENT WITH ACTIVE FLOW CONTROL BY SUCTION

Vehicle model	Pressure coefficient, Cp		Increasing Cp, (%)
	Without active flow control	With suction	
$\theta=25^0$	-1.1148	-0.9616	13.74
$\theta=30^0$	-1.0716	-1.0442	2.57
$\theta=35^0$	-1.3556	-0.9964	26.50

III.1. The Computational Approach

Table V shows aerodynamic drag coefficient for computational approach on the three vehicle models with front slant angle of θ=25°, θ=30° and θ=35° without active control and with active control with suction speed U_{sc} of 0.5 m/s and upstream velocity U_o of 16.7 m/s.

On the other hand, the relationship of aerodynamic drag and slant angle is presented in Figure 7.

TABLE V
AERODYNAMIC DRAG COEFFICIENT BY COMPUTATIONAL APPROACH

Vehicle model	Aerodynamic drag coefficient, C_d	
	Without active flow control	With suction
θ=25^0	1.7752	1.5248
θ=30^0	1.6709	1.5434
θ=35^0	1.7556	1.4968

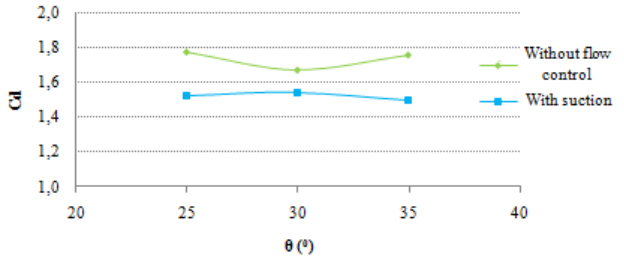

Fig. 7. Relationship of aerodynamic drag and slant angle of front part of vehicle model by computational approach

From Table VI and Figure 7, some information are obtained that, in vehicle model without active control, the smallest aerodynamic drag coefficient is gained in model with slant angle θ=30° with the value of 1.6709 while on the models with θ=25° and θ=30° aerodynamic drag coefficients were 1.7752 and 1.7556 respectively. With the addition of active control by suction, it is shown that the aerodynamic drag coefficients on each model were decreasing.

The smallest drag coefficient occurred in the model with applied active control by suction with θ=35° with the value of 1.4968 while for models with θ=25° and θ=30° were 1.5248 and 1.5434 respectively.

TABLE VI
AERODYNAMIC DRAG REDUCTION WITH ACTIVE FLOW CONTROL BY SUCTION BY COMPUTATIONAL APPROACH

Vehicle model	Aerodynamic drag reduction, %
θ=25^0	14.11
θ=30^0	7.63
θ=35^0	14.74

From Table VI, information is obtained that the reduction of the largest aerodynamic drag as the effect of active control by suction with suction velocity U_{sc}=0.5 m/s and upstream velocity U_o = 16.7 m/s on vehicle model with θ of 35° was 14.74% while for the vehicle model with θ= 25°and 30° the reduction were 14.11% and 7.63% respectively.

The value of aerodynamic drag on test model with slant angle at front θ=35° as the effect of active control by suction application is capable to increase pressure coefficient on rear part of vehicle model to 26.50%. The increasing of pressure coefficient on rear part on vehicle model can reduce the aerodynamic drag. Results obtained from the research has confirmed the results gained by other researchers [15], [20], [21], [22] where the application of active control by suction can decrease aerodynamic drag on vehicle models.

III.2. The Experimental Approach

Table VII shows aerodynamic drag coefficients from experimental approach on three vehicle models, the same model used for computational approach. The relationship of aerodynamic drag coefficients to slant angle of front part of vehicle is presented in Figure 8.

TABLE VII
AERODYNAMIC DRAG COEFFICIENT BY EXPERIMENTAL APPROACH

Vehicle model	Aerodynamic drag coefficient, Cd	
	Without active flow control	With suction
θ=25^0	1.6237	1.4071
θ=30^0	1.5173	1.4160
θ=35^0	1.5655	1.3530

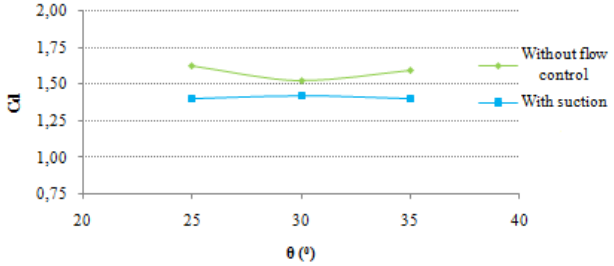

Fig. 8. Relationship of aerodynamic drag and slant angle of front part of vehicle model by experimental approach

Information obtained from Table VII and Figure 8 is that on vehicle models without flow control, the smallest aerodynamic drag coefficients occured in the model with θ=30° with the value of 1.5173 while on vehicle models with θ=25° and θ=30° the coefficients were 1.6237 and 1.5655 respectively.

Additional active control by suction give results that all models underwent reduction of aerodynamic drag coefficients. The smallest aerodynamic drag coefficients occured in the model with θ=35° with the value of 1.3530 while on vehicle models with θ=25° and θ=30° the coefficients 1.4071 and 1.4160 respectively. Obtained value from experiments have similar tendency to that from computational approach.

The reduction of aerodynamic drag on models with active control by suction is shown on Table VIII. From the table, it is obvious that the smallest reduction of aerodynamic drag by active control with suction speed U_{sc} of 0.5 m/s and upstream velocity U_o of 16.7 m/s occurred on the model with θ=35° giving the reduction of 13.57% while on models with θ=25° and θ=30° the reductions were 13.34% and 6.68% respectively.

TABLE VIII
AERODYNAMIC DRAG REDUCTION WITH ACTIVE FLOW CONTROL BY SUCTION BYEXPERIMENTAL APPROACH

Vehicle model	Aerodynamic drag reduction, %
θ=25^0	13.34
θ=30^0	6.68
θ=35^0	13.57

The comparison of aerodynamic drag coefficients obtained from computational and experimental approach

from vehicle models with θ=25°, θ=30° and θ=35° are shown on Tables IX, X and XI respectively.

The comparison of aerodynamic drag coefficient from computational and experimental approach for θ=25° model is shown in Table IX.

TABLE IX
COMPARISON AERODYNAMIC DRAG COEFFICIENT (CD) FOR VEHICLE MODEL WITH $\theta=25^0$

Description	Aerodynamic drag coefficient, (Cd)		Aerodynamic drag coefficient (Cd) reduction (%)
	Without flow control	With flow control by suction	
Computational	1.7752	1.5248	14.11
Experiment	1.6237	1.4071	13.34
Difference	8.53%	7.72%	0.77

It can be seen that the coefficients of aerodynamic drags of the two approaches for models without flow control differ in about 8.53%. For models with active control by suction at suction speed of 0.5 m/s, the two approaches give 7.72% difference in aerodynamic drag coefficient values. It is also shown that the reduction of aerodynamic drag coefficient for the two approaches differs only 0.77%.

The comparison of aerodynamic drag coefficient for vehicle model with θ=30° is shown in Table X. The comparison of aerodynamic drag coefficient from computational and experimental approaches for θ=30° model is shown in Table X.

The coefficients of aerodynamic drag of the two approaches for models without flow control have 9.19% differences. For vehicle models with active control by suction at suction speed of 0.5 m/s, the two approaches give 8.25% difference in aerodynamic drag coefficient values.

The table also shows that the reduction of aerodynamic drag coefficients between computational and experimental approaches differ on only 0.95%.

TABLE X
COMPARISON AERODYNAMIC DRAG COEFFICIENT (CD) FOR VEHICLE MODEL WITH $\theta=30^0$

Description	Aerodynamic drag coefficient, (Cd)		Aerodynamic drag coefficient (Cd) reduction (%)
	Without flow control	With flow control by suction	
Computational	1.6709	1.5434	7.63
Experiment	1.5173	1.4160	6.68
Difference	9.19%	8.25%	0.95

Aerodynamic drag coefficients from computational and experimental approaches for θ=35° model are listed in Table XI. For models without flow control, the coefficients of aerodynamic drag of the two approaches for have 10.82% differences.

For vehicle models with active control by suction at suction speed of 0.5 m/s, the two approaches give 9.61% difference in aerodynamic drag coefficient values. The table also shows that the reductions of aerodynamic drag coefficients of the two approaches differ about 1.17%.

TABLE XI
COMPARISON AERODYNAMIC DRAG COEFFICIENT (CD) FOR VEHICLE MODEL WITH $\theta=35^0$

Description	Aerodynamic drag coefficient, (Cd)		Aerodynamic drag coefficient (Cd) reduction (%)
	Without flow control	With flow control by suction	
Computational	1.7556	1.4968	14.74
Experiment	1.5655	1.3530	13.57
Difference	10.82%	9.61%	1.17

IV. Conclusion

From the analysis of pressure coefficients and drag reduction on vehicle models with frontal slant angles (θ) of 25°, 30° and 35° due to the application of active flow control by suction it can be concluded:

a. Active flow control by suction and variations on front geometry give significant impact to the increasing of pressure coefficients and reduction of aerodynamic drag.
b. The largest increasing on pressure coefficients occurred on vehicle model with θ=35° with the value of 26.50%, where pressure coefficients without and with active control by suction on 0.5 m/s speed were -1.3556 and -0.9964 respectively.
c. The largest reduction of aerodynamic drag occurred on vehicle model with θ=35° with the value of 14.74 for computational approach and 13.57 for experimental approach, while the reductions of aerodynamic drag coefficients of the two approaches differ about 1.17%.

Acknowledgements

The research was funded by the Ministry of Research, Technology and Higher Education through University Excellence Scheme F.Y 2017, with Research Contract No. : 2774/UN4.21/LK23/2017, dated May 4th2017.

References

[1] Ahmed, S. R., G. Ramm, and G. Faltin, (1984) Some Salient Features of the Time Averaged Ground Vehicle Wake, *SAE Paper* No. 840300.
[2] Han, T., (1989) Computational Analysis of Three-Dimensional Turbulent Flow around a Bluff Body in Ground Proximity, *AIAA J.*, Vol. 27(9), pp. 1213–1219.
[3] Hucho, W.H., (1998), Aerodynamics of Road Vehicles, 4th edition, SAE International, Warrendale, PA.
[4] Gilliéron, P., and A .Kourta, (2009), Aerodynamic Drag Reduction by Vertical Splitter Plates, *Exp. Fluids*, Vol. 48(1), pp. 1–16.
[5] Aider, J.L., J.F. Beaudoin, and J.E. Wesfreid, (2010) Drag and Lift Reduction of a 3D Bluff-Body Using Active Vortex Generators, *Exp. Fluids*, Vol. 48(5), pp. 771–789.
[6] Gillieron, P., (2003), Detailed Analysis of the Overtaking Process, *J. Mech. Eng.*, Vol. 53, pp. 1-17.
[7] Aider J.L., .F. Beaudoin, and J.E. Wesfreid (2009) Drag and Lift Reduction of a 3D Bluff-Body using Active Vortex Generators, *Experimental in Flui*ds, Springer.
[8] Gilliéron P. and A. Kourta, (2010) Aerodynamic drag reduction by vertical splitter plates, *Experimental in Fluids*, Vol. 48, pp. 1–16.
[9] Fourrie G, L. Keirsbulck, L. Labraga& P. Gilliéron, (2011) Bluff-body drag reduction using a deflector, *Experimental in*

Fluids, Vol. 50, pp. 385–395.
[10] Hinterberger C., M.G. Villalba& W. Rodi, (2004) Large eddy simulation of flow around the Ahmed body, Institute for Hydromechanics, University of Karlsruhe, Germany.
[11] Fares E., (2006) Unsteady flow simulation of the Ahmed reference body using a lattice Boltzmann approach, *Computers and Fluids*, Vol. 35, pp. 940-950.
[12] Minguez M., R. Pasquetti& E. Serre, (2008) High-order Large Eddy Simulation of Flow over the Ahmed Body" Car Model, *Physics of Fluids*, pp. 20.
[13] Uruba V., and O. Hladík, (2009) On the Ahmed Body Wake, Colloquium Fluid Dynamics, Institute of Thermomechanics AS CR, v.v.i., Prague.
[14] Conan B., J. Anthoine, and P. Planquart, (2011) Experimental aerodynamic study of a car-type bluff body, *Experimental in Fluids*, Vol. 50, pp. 1273–1284.
[15] Roumeas M, P. Gilliéron, A. Kourta, (2009) Drag reduction by flow separation control on a car after body, *International Journal for Numerical Methods in Fluids*,Vol. 60, pp.1222- 1240.
[16] Krogstad, P.A. and A. Kourakine, (2000) Some effects of localized injection on the turbulence structure in a boundary layer", *Phys. Fluids*, Vol.12, pp. 2990–2999.
[17] Park, J, H. Choi, (1999) Effects of uniform blowing through blowing or suction from a spanwise slot on a turbulent boundary layer flow", *Phys. Fluids*, Vol. 11, pp. 3095–3105.
[18] Sano, M. and N. Hirayama, (1985) Turbulent boundary layer with injection and suction through a slit", *Bull JSME*, Vol. 28, pp. 807–814.
[19] Brunn A., E. Wassen, D. Sperber, W. Nitsche, and F. Thiele, (2007) Active Drag Control for a Generic Car Model, *Active Flow Control*, NNFM 95, pp. 247–259.
[20] Harinaldi, Budiarso, Warjito, E.A. Kosasih, R. Tarakka, S.P. Simanungkalit, (2012) Active technique by suction to control the flowstructure over a van model, *Journal of Engineering and Applied Science*, Vol. 7 (2), pp.215-222.
[21] Harinaldi, Budiarso, R. Tarakka, S.P. Simanungkalit, (2011) Computational Analysis of Active Flow Control to Reduce Aerodynamics Drag on a Van Model. *International Journal of Mechanical & Mechatronics Engineering IJMME-IJENS*, Vol. 11 (03), pp. 24-30.
[22] Harinaldi, Budiarso, R. Tarakka, S.P. Simanungkalit, (2013) Effect of Active Control by Blowing to Aerodynamic Drag of Bluff Body Van Model, *International Journal of Fluid Mechanics Research*, Vol. 40 (4), pp. 312-323.
[23] Tarakka R, Jalaluddin, B. Mire, M.N. Umar, (2015) Effect of Turbulence Model In Computational Analysis of Active Flow Control on Aerodynamic Drag of Bluff Body Van Model, *International Journal of Applied Engineering Research*, Vol. 10, Number 1 pp. 207-219.
[24] Anderson, J.D., (2001) *Fundamental of Aerodynamics* (3rded), Singapore, McGraw-Hill.
[25] Gilliéron, P. and A. Sphon, (2002) Flow separations generated by simplified geometry of an automotive vehicle, *IUTAM Symp. Steady Separated Flow*.

Authors' information

[1]Hasanuddin University.

[2]Sekolah Tinggi Teknik Baramuli.

Rustan Tarakka, born in Pinrang on August 27th 1975 is a Lecturer in the Department of Mechanical Engineering, Faculty of Engineering, Hasanuddin University, Makassar, Indonesia. He holds a doctoral degree from University of Indonesia, Jakarta, Indonesia. His research areas are on fluid dynamics and computational fluid dynamics. Dr. Rustan is a member of the Institutions of Engineers Indonesia.

Nasaruddin Salam, born in Bulukumba on December 20th 1959 is a Professor and the Chairman of Fluid Mechanics Laboratory in Department of Mechanical Engineering, Faculty of Engineering, Hasanuddin University Makassar Indonesia. He holds a doctoral degree from Brawijaya University, Malang Indonesia. His research fields include fluid dynamics particularly on tandem bodies. Prof. Nasaruddin Salam is a member of the Institutions of Engineers Indonesia.

Jalaluddin, born in Sompu on August 25th 1972 obtained a Doctor of Engineering in Mechanical Engineering in 2012 from Saga University Japan. He is an Associate Professor of Mechanical Engineering of Hasanuddin University, Makassar, Indonesia. His area of research covers Ground Heat Exchanger for Space Conditioning System, Renewable Energy focus on Solar Energy including Solar Water Heating System and Photovoltaic Applications. Dr-Eng. Jalaluddin is a member of Institutions of Engineers Indonesia.

Muhammad Ihsan, born in Watampone, February 20th 1977, is a lecturer on Sekolah Tinggi Teknik Baramuli, Pinrang, Indonesia. He graduated from Hasanuddin University with a bachelor in engineering. He also holds master degrees in transport engineering from Asian Institute of Technology, Bangkok, Thailand and Universitas Gajah Mada, Yogyakarta, Indonesia. His research interests include transport engineering, fluid mechanics and hydraulics. Mr. Muhammad Ihsan is a member of Institutions of Engineers Indonesia.